Renewable Energy 35 (2010) 2325–2334

Contents lists available at ScienceDirect

Renewable Energy

journal homepage: www.elsevier.com/locate/renene

Three-dimensional effects and arm effects on modeling a vertical axis tidal current turbine

Ye Li [a,*,1], Sander M. Calisal [b,c]

[a] National Wind Technology Center, National Renewable Energy Laboratory, 1617 Cole Blvd, MS 3811, Golden, CO 80401, USA
[b] Department of Mechanical Engineering, The University of British Columbia, Vancouver, Canada
[c] The Piri Reis University Turkey, 34940 Tuzla, Istanbul, Turkey

ARTICLE INFO

Article history:
Received 25 September 2009
Accepted 3 March 2010
Available online 18 April 2010

Keywords:
Tidal current energy
Three-dimensional effects
Arm effects
Towing tank test

ABSTRACT

Three-dimensional effects in studying a vertical axis tidal current turbine are modeled using a newly developed vortex method. The effects on predicting power output and wake trajectory are analyzed in particular. The numerical results suggest that three-dimensional effects are not significant when the height of the turbine is more than seven times the turbine radius. Further discussions are presented focusing on the relationship between the turbine height and the angle of attack and the induced velocity on a blade of the turbine without arms. Besides the three-dimensional effects, arms effects are quantified with an analytical derivation of the polynomial formula of the relationship between arm effects and the tip speed ratio of the turbine. Such a formula provides a correction for existing numerical models to predict the power output of a turbine. Moreover, a series towing tank tests are conducted to study the three-dimensional effects as well as the arm effects. Good agreements are achieved between the results obtained with numerical calculations with the arm effects correction and the towing tank tests. Finally, three-dimensional effects are examined experimentally together with the arm effects by using an end-plate test, which suggests that the combinational effect is rather minimal. For turbine designers at the early design stage, we recommend that a two-dimensional model is acceptable considering the high cost of the three-dimensional model.

1. Introduction

This paper reports a recent investigation on exploring the three-dimensional effects and arm effects in modeling a vertical axis tidal current turbine. A tidal current turbine is in principle similar to a wind turbine. Considerable power can be generated from tidal currents and in-stream flows by such turbines. These flows are regarded as one of the most promising alternative energy resources, given the fact that traditional energy resources are being depleted and have significant negative environmental impacts [1]. Naturally, tidal current turbines have received wide attention from scholars in different disciplines, e.g., oceanography [2], industrial engineering [3], environmental sciences [4], and ocean engineering [5–7]. A vertical axis turbine means that the turbine's blades rotate in the vertical plane (Fig. 1). From now on, when tidal current turbine is mentioned, it is referred to vertical axis tidal current turbine.

1.1. Numerical methods

In the ocean engineering community, the standard approaches to evaluate a turbine are experimental tests and numerical simulation. Because of the high cost of experimental tests, large efforts have been put on developing numerical simulation methods, especially since the 1980s when high-speed computational technologies became widely available. These numerical models have evolved from one-dimensional [8], two-dimensional [9], and then to three-dimensional models [10–12]. Of course, a three-dimensional model can provide a better accuracy than a two-dimensional model. However, computational tasks for the three-dimensional model lead to a considerable high cost. The computational cost of three-dimensional models is at least 30 times higher than that of two-dimensional models to simulate a turbine. At early design stage, the standard procedure is that designers optimize the configuration (e.g., blade profile and turbine's diameter) after roughly evaluating the turbine's performance (e.g., power output and torque fluctuation) with a certain configuration [7]. Consequently, many designers prefer to use a two-dimensional model for power estimation. Technically, such a preference must be justified by evidences showing that the results predicted by two-dimensional models are

* Corresponding author. Tel.: +1 303 384 6988.
E-mail address: ye.li@nrel.gov (Y. Li).
[1] This work is conducted when Ye Li was with University of British Columbia Ye Li now a senior research scientist at National Wind Technology Center, National Renewable Energy Laboratory.

0960-1481/$ – see front matter © 2010 Elsevier Ltd. All rights reserved.
doi:10.1016/j.renene.2010.03.002

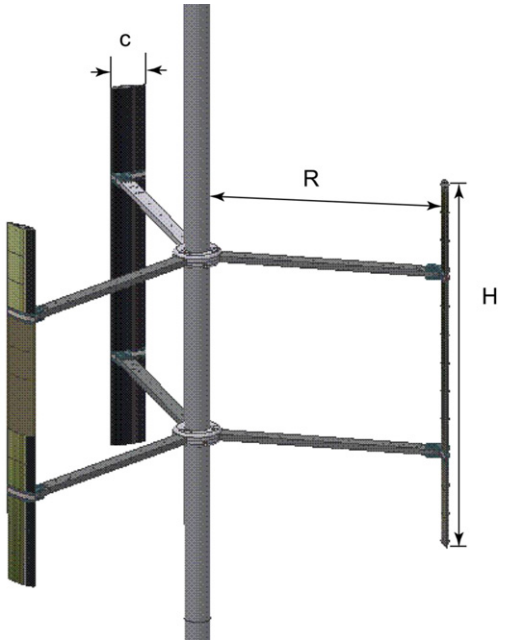

Fig. 1. The sketch of a vertical axis tidal current turbine (H: turbine height; R: turbine radius; c: blade chord length).

comparable to the results obtained with three-dimensional models. In other words, there must be evidences showing that the three-dimensional effects are not significant.

1.2. Objective

The main purpose of this paper is to investigate the three-dimensional effects by comparing the two-dimensional results and three-dimensional results. In Section 2, after presenting the difference between two-dimensional and three-dimensional models, we analyze the relationships between the turbine height and the power output and between turbine height and wake trajectory, and compare the wake trajectory and power output of a tidal current turbine obtained with two-dimensional and three-dimensional models. Moreover, we analyze the angle of attack and induced velocity along the blade span, which provides more theoretical insight into the three-dimensional effects. In Section 3, we present a series of experimental tests for quantifying the arm effects, and develop an arm effects correction formula. Additionally, we present a series of end-plate tests for studying the three-dimensional effect with arms. Finally, conclusions and future work are presented in Section 4. The findings in this study suggest that three-dimensional effects are negligible when the turbine height is over seven times the turbine radius and the accuracy of the results obtained with the arm effects correction formula is quite acceptable.

2. Numerical analysis of three-dimensional effects

In this study, we consider the turbine in an ideal flow, i.e., open water, no bottom no turbulence and no free surface. Many numerical methods are used to develop both two-dimensional and three-dimensional models, e.g., boundary element method [13], finite element method [10], vortex method [11] and Reynolds Averaged Navier–Stokes(RANS) [10]. It is understood that RANS can provide an accurate result but it is too costly. Among rest methods, vortex method and boundary element method are the most cost-effective. The vortex method is more suitable for simulating a turbine's behavior with the rotation of the turbine and the unsteady wake and the boundary element method can provide a more detailed description of force and pressure on the blade surface. In this study, our focus is to study the main characteristics of the turbine (i.e., power output and wake velocity) while we do not study the cavitation of the blade or other features related to the blade surface; thus, we use a newly developed vortex method, DVM-UBC, to develop both two-dimensional and three-dimensional models and study the three-dimensional effects.

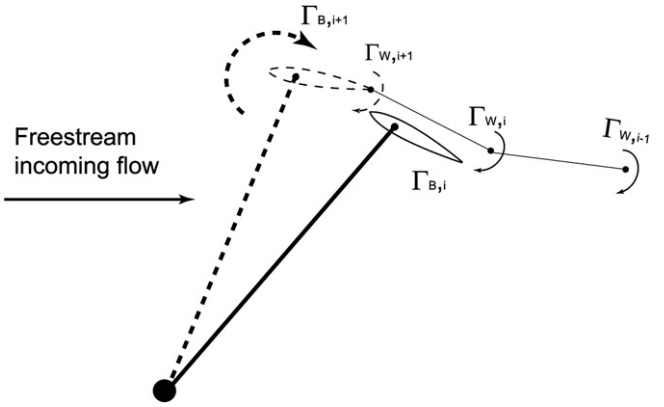

Fig. 2. An illustration of a two-dimensional time-dependent (unsteady) vortex wake structure.

DVM-UBC is a discrete vortex method for simulating underwater structures with unsteady flow-through proposed by Li and Calisal [11]. DVM-UBC is a fully three-dimensional method. Each blade is represented by a set of vortices filaments with an accurate description of the blade curvature.[2] Similarly, one set of free vortices filaments together with uniform flow is used to represent the unsteady flow. The wake free vortices are shed from the blade tip in each time step, as DVM-UBC is a time-dependent method. In each time step, DVM-UBC utilizes the relationship between the strength of free vortex and induced velocity to approximate flow and to predict lift, and uses this relationship together with viscous effect to predict drag. Compared with previous discrete vortex methods, e.g., [14], DVM-UBC introduces viscous effects into its formulation by simulating the wake vortices from their appearance to their disappearance. The physics of water is well represented. The computational stability problems is well discussed as well. Furthermore, good agreement have been obtained between the experimental results and the numerical results obtained with DVM-UBC [12]. In this section, we briefly recapitulate the formulation of DVM-UBC, before we discuss the specific difference between two-dimensional modeling and three-dimensional modeling; readers who are interested in the details of modeling and validation of the DVM-UBC are referred to Li and Calisal [11,12]. Basically, the primary difference of a two-dimensional model and three-dimensional model is the representation of the wake and the blade, and it is reviewed here. The blade in the two-dimensional modal is described as two-dimensional foil. The strength of the two-dimensional wake vortices, as depicted in Fig. 2, can be written as (1).

$$\Gamma_{W,i} = \Gamma_{B,i} - \Gamma_{B,i-1} \tag{1}$$

[2] Some turbines' blade is curved, e.g., helical blade or Darrieus type.

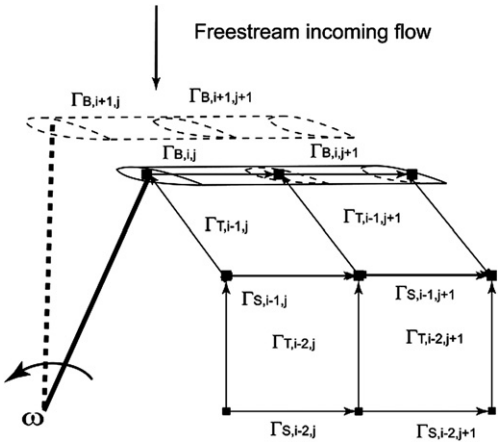

Fig. 3. An illustration of a three-dimensional time-dependent (unsteady) vortex wake structure (redrawn from Li and Calisal [12]).

where $\Gamma_{W,i}$ and $\Gamma_{B,i}$ denote the strengths of wake vortex and blade bound vortex at time step i, respectively.

In a three-dimensional model, each blade is described as a number of blade elements. The vortex system of each element is assumed to be of a horseshoe shape initially, and it is divided into two types of wake vortices which are the spanwise vortex and trailing edge vortex (Fig. 3). The strength of the spanwise vortex filament, Γ_S, and strength of the trailing edge vortex shedding filament, Γ_T, can be expressed as follows,

$$\Gamma_{S,i-1,j} = \Gamma_{B,i-1,j} - \Gamma_{B,i,j} \tag{2}$$

$$\Gamma_{T,i-1,j} = \Gamma_{B,i,j} - \Gamma_{B,i,j-1} \tag{3}$$

where i is the index of the time step and j is the index of the blade element.

Theoretically, these wake vortices affect the performance of a turbine by inducing induced velocities on the blade. According to Biot–Savart law [15], given a vortex filament of an arbitrary shape with a strength Γ and a length l (e.g., a turbine blade), the induced velocity at point p (but not on the filament) can be calculated in its three-dimensional format by using (4) and in its two-dimensional format by using (5),

$$\vec{U}_{iP,l} = \frac{\Gamma}{4\pi}\int_l \frac{\vec{r}\times d\vec{l}}{r^3} \tag{4}$$

$$\vec{U}_{iP} = \frac{\Gamma}{2\pi r} \tag{5}$$

where $\vec{r}$ denotes the position vector from a point on the filament to point p. Then, the totally induced velocity on the blade induced by the wake vortices can be obtained by using either (6) for the three-dimensional model or (7) for the two-dimensional model.

$$\vec{U}_{\text{induced,3D}} = \sum_i \sum_j \frac{\Gamma_{T,i,j}}{4\pi}\int_{l_{i,j}} \frac{\vec{r_{i,j}}\times d\vec{l}}{r_{i,j}^3} + \sum_i \times \sum_j \frac{\Gamma_{S,i,j}}{4\pi}\int_{l_{i,j}} \frac{\vec{r_{i,j}}\times d\vec{l}}{r_{i,j}^3} \tag{6}$$

$$\vec{U}_{\text{induced,2D}} = \sum_i \frac{\Gamma_{W,i}}{2\pi r_i} \tag{7}$$

Additionally, in order to simplify the analysis, we nondimensionalize all the parameters. Besides using the power coefficient to represent the power output of a turbine, we select U_∞ (incoming flow velocity), R (turbine radius) and ρ_w (water density) as independent variables to nondimensionalize other parameters. For example, we have dimensionless velocity and length by using (8) and (9), respectively.

$$\forall U\ (\text{velocity}),\ \text{we have}\ \hat{U} = \frac{U}{U_\infty} \tag{8}$$

$$\forall l\ (\text{length}),\ \text{we have}\ \hat{l} = \frac{l}{R} \tag{9}$$

2.1. Power output and wake trajectory

A standard procedure to validate a numerical method is to conduct kinematic analysis and dynamic analysis. When designers are evaluating a tidal current turbine, they usually evaluate the turbine's performance (e.g., power output) and environmental impacts (e.g., wake fluctuation [7]). Power output is a dynamic result and an indicator of the performance of a turbine, and wake trajectory is a kinematic result and an indicator of the environmental impact of the turbine. Hence, we analyze the power output and the wake trajectory of tidal current turbines in both two-dimension and three-dimension so as to study the three-dimensional modeling's impacts on the prediction of the performance and environmental impacts.

2.1.1. Power output

Firstly, we compare the power coefficients obtained by using the numerical models (both two-dimensional and three-dimensional) with the experimental results reported by Templin [16]. The basic specifications of the turbine are that the turbine is a one-blade turbine, the blade type is NACA0015 (curved blade, the detailed curvature can be found in Templin [16]), the solidity (Nc/R, where N and c denote the number of the blades and the length of blade chord, respectively) is 0.08333, the height to radius ratio is 2, and the Reynolds number(with respect to the blade chord length) is 360,000. The comparison in Fig. 4 shows the power coefficient with respect to with respect to tip speed ratio (TSR $= R\omega/U_\infty$, where ω

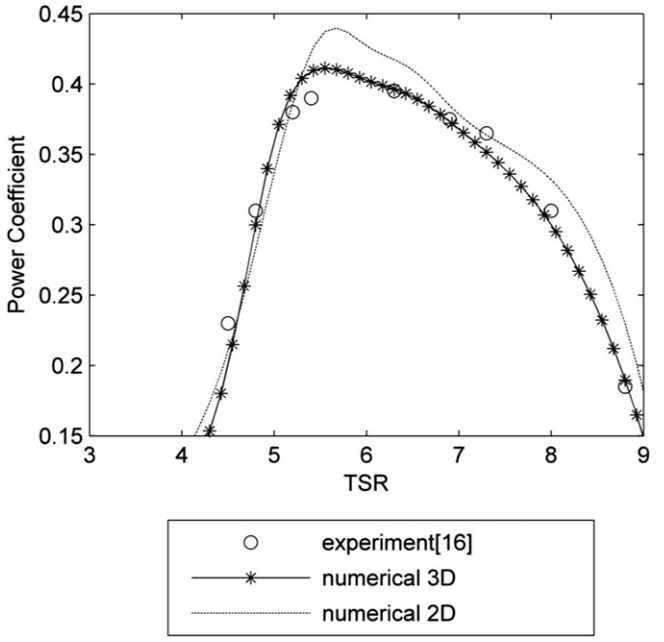

Fig. 4. Comparison of power coefficients of an example turbine obtained with different methods.

denotes turbine angular velocity). It suggests that both numerical results are comparable to the experimental results. It also shows that the maximum power coefficient of an ideal turbine, i.e., the maximum power coefficient obtained with the two-dimensional model is 0.447. Such a power coefficient is a few percent higher than that of the experimental result while that obtained with the three-dimensional model is a few percent lower than that of the experimental result. The difference between the three-dimensional results and the experimental results may be caused by the approximation of the blade curvature in the numerical model.

We quantify the three-dimensional effects on power coefficient by simulating turbines with different heights while keeping the other specifications the same as those stated above (Fig. 5). It is noted that when the height is more than six times the turbine radius, the maximum power coefficient increases much more slowly with respect to the turbine height. The maximum power coefficient of a three-dimensional turbine, the height of which is more than six times turbine radius, is more than 0.43, which is more than 95% of that of a two-dimensional turbine. Thus, one can say that the three-dimensional effect on power coefficients is not significant when the turbine height to radius ration is more than six.

2.1.2. Wake trajectory

We compare the wake trajectories of a turbine obtained with the numerical models (both two-dimensional and three-dimensional) with the experimental results reported by Strickland [17]. The specifications of the turbine include that the blade is NACA0012 (straight blade), TSR is equal to 5, the height to radius ratio is 2, the solidity is 0.45, and the Reynolds number is 80,000. Because of the similarity between the wake trajectory obtained with the two-dimensional model and the wake's projection on the horizontal plane obtained with the three-dimensional model, we only show the projection of the three-dimensional wake trajectory on the horizontal plane (Fig. 6). We calculate the deviation of results obtained with numerical methods from the experimental results with respect to the turbine radius. In order to systematically study the deviation, we compare the values of the first five cross-x-axis points(i.e., the x values of the points, the y values which are zero), which are x_1, x_2, x_3, x_4 and x_5, and the values of the four extreme y points in the first two revolutions(i.e., the maximum and minimum y value of each revolution), which are y_1, y_2, y_3 and y_4, e.g. we calculate $(x_1(\text{numerical}) - x_1(\text{experimental}))/R$. The deviations are presented in Table 1. In general, the results generated with both the three-dimensional model and the two-dimensional model are comparable with the experimental results. The difference between the experimental results and the results generated with the three-dimensional model is within 5%, and the difference between the experimental results and the results generated with the two-dimensional model is within 8%.

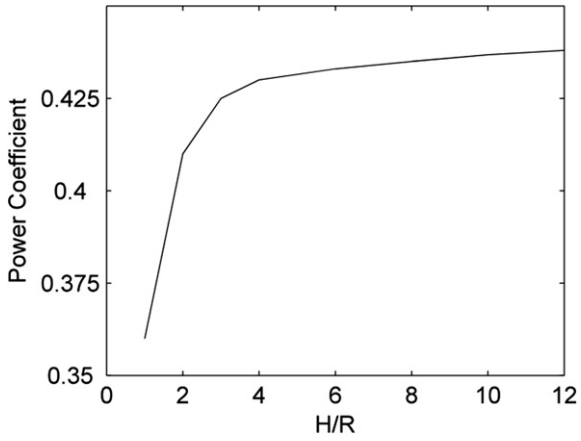

Fig. 5. The relationship between turbine height and maximum power coefficient.

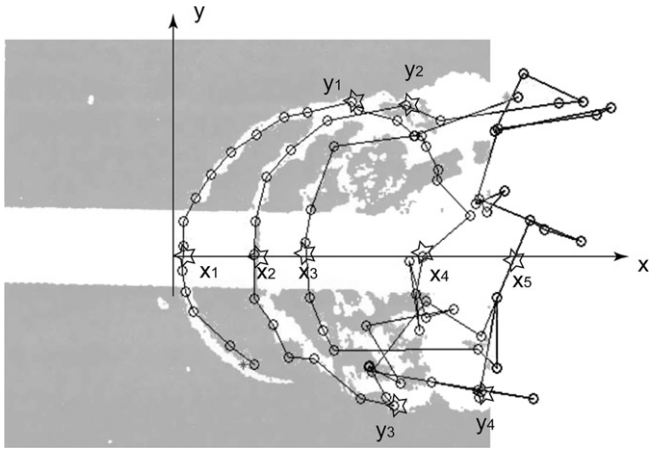

Fig. 6. Two-dimensional wake comparison of a three-blade turbine (dash-circle: numerical result; white bubble: Strickland [17]).

We then investigate the three-dimensional effects by analyzing the deviation of the results obtained with the three-dimensional model from the two-dimensional model with respect to the radius at different turbine heights. Here, we calculate $|x_i(\text{three}-\text{dimensional}) - x_i(\text{two}-\text{dimensional})|/R$. The results suggest that the deviations tend to be constant when the turbine's height is over seven times turbine radius (Fig. 7). Thus, one can say that the three-dimensional effects on the wake trajectory of the turbine are not significant when the turbine height is over seven times turbine radius.

We have analyzed the three-dimensional effects on the horizontal plane. Here, we analyze the maximum relative elevation (i.e., $\max|\delta z|/R$) of the wake trajectory from the location where the wake vortices are shed in the vertical plane. For illustration purposes, we show the first two cycles of the wake trajectory from a blade's mid-span (Fig. 8), and the specifications of the turbine are the same as that in the horizontal wake analysis. We find that the relative elevation of the first cycle is 1.4% and that of the second cycle is 3.6%. Similarly, we investigate turbines with different heights. Fig. 9 shows the relationship between the maximum relative elevations from two locations (i.e., mid-span and blade tip) and the turbine heights. The more the wake cycles are developed, the higher the elevation is. However, a high elevation does not increase the three-dimensional effects because the strength of the wake vortices farther downstream (e.g., in the eighth cycle) is much less than that of the wake vortices in the first couple of cycles. One can notice that the three-dimensional effects on the elevation are not significant when the turbine height is more than six times the turbine radius. Furthermore, it is noted that the elevation of the wake from the blade tip is much greater than that from mid-span. This is primarily because the wake from the blade tip is affected by both trailing edge wake vortices and spanwise wake vortices at blade tips while the wake from the mid-span is affected by a quasi

Table 1
The relative deviation of the results with numerical models from the experimental results.

Model	x_1	x_2	x_3	x_4	x_5	y_1	y_2	y_3	y_4
3-D	−1.9%	1.1%	−0.8%	−4.2%	−2.1%	−0.7%	−1.8%	3.3%	−3.6%
2-D	2.6%	−1.8%	1.1%	2.5%	3.4%	2.7%	2.4%	7.4%	6.1%

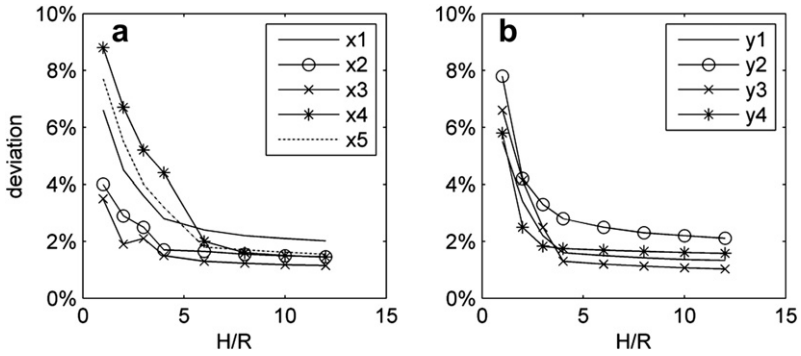

Fig. 7. The deviation of significant points: a) $|x_i(\text{three}-\text{dimensional}) - x_i(\text{two}-\text{dimensional})|/R$, and b) $|y_i(\text{three}-\text{dimensional}) - y_i(\text{two}-\text{dimensional})|/R$.

symmetric trailing edge wake. Moreover, three-dimensional effects on the blade tip will be analyzed in Section 2.2 in greater details by studying the induced velocity and angle of attack(AOA).

2.2. Induced velocity and angle of attack

The power output and wake of a tidal current turbine are determined by the change of the circulation of the blade, which is significantly affected by the unsteady wake via the induced velocity on the blade and the angle of attack (AOA). Therefore, we conduct a more fundamental analysis about the three-dimensional effects by studying the induced velocity and AOA along the blade span. Specifically, we study a straight blade turbine, the specification of which includes that the blade is NACA0015, the solidity is 0.375, TSR is 4.75, and the Reynolds number is 200,000. Fig 10 shows the induced velocities and AOA at five locations of a blade (i.e., blade tip, 20%, 40%, 60% and 80% of the span) and of the corresponding two-dimensional turbine. One may notice that the differences between the induced velocities at the blade tip and those of the two-dimensional results are much larger than the difference of the induced velocities at other locations and those of the two-dimensional results. Similar feature is observed for AOA. These results suggest that the three-dimensional effects are primarily at the blade tip. We also find that the taller the turbine is, the less the deviation of the three-dimensional results from the two-dimensional results are. That is to say, for a very tall turbine (e.g., when the height of the turbine is more than seven times the radius of the turbine), the three-dimensional effects can be neglected. On the contrary, for a practical turbine, e.g., the height of which is one to two times the turbine radius, the three-dimensional effects will significantly affect its power output. One may modify the blade tip to obtain better performance. For example, one can install an end-plate, which is analyzed in detail in Section 3.4.

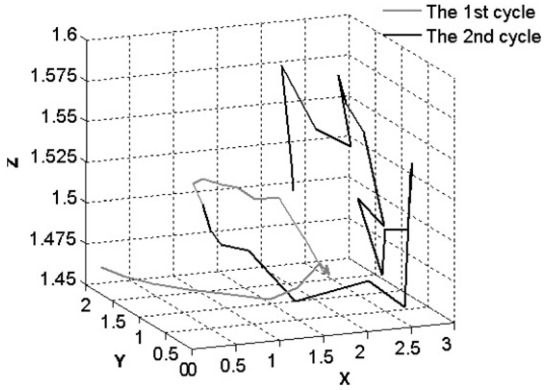

Fig. 8. Wake trajectory of the first two cycles of a three-blade turbine (TSR = 4.75, H/R = 2).

Additionally, because of the turbine rotation, the unsteady wake is asymmetric with respect to the plane where the azimuth angle is zero (Fig. 6). Consequently, the AOA and the induced velocity are asymmetric too. Furthermore, for turbines with different height to radius ratios, one can observe a shift of the AOA and induced velocities with respect to the azimuth angle. Such a feature suggests that the three-dimensional effect will affect the asymmetry of the characteristics (e.g., wake, force and torque) along the span, although this feature is not noticeable when the turbine is very tall.

Above discussions all focus on the height to radius ratio, one may also concern about the aspect ratio. For the straight blade application studied in this paper, the aspect ratio can be written as c/H. In this case, we can derive the impact of aspect ratio from the impact of height to radius ratio and solidity. It is understood that the aspect ratio is proportional to the product of solidity and radius to height ratio, i.e. $c/H \propto Nc/R \times R/H$. Thus, when solidity, a two dimensional coefficient, is fixed, the impact of the aspect ratio on the three-dimensional effect is the opposite of the impact of the height to radius ratio. For those blades with curvature and with twist, we shall conduct a further investigation.

3. Arm effects

The arms are not simulated in the numerical methods as reviewed in Section 1. However, a real vertical axis tidal turbine always has arms that connect the blade with the shaft to support the structure. Arms inevitably affects the power output of a turbine by adding additional drag on the turbine and inducing hydrodynamic interactions among arms, shaft and blades. By using a perturbation theory, e.g., Van Dyke [18], we can calculate the power coefficient of a turbine as follows,

$$C_P = C_{P,B} + C_{P,AS} + C_{P,INT} \tag{10}$$

where $C_{P,B}$, $C_{P,AS}$ and $C_{P,INT}$ denote the power coefficients contributed by the blades, the arms and shaft, and the interactions among blade, arms and shaft, respectively. Theoretically, the interactions term is a higher order term and is much less than those first order terms. Thus, we only keep the first order terms and rewrite (10) as follows,

$$C_P \approx C_{P,B} + C_{P,AS} \tag{11}$$

3.1. Experimental setup

We conducted a series of experimental tests to the performance of several turbines. These tests were conducted in the towing tank

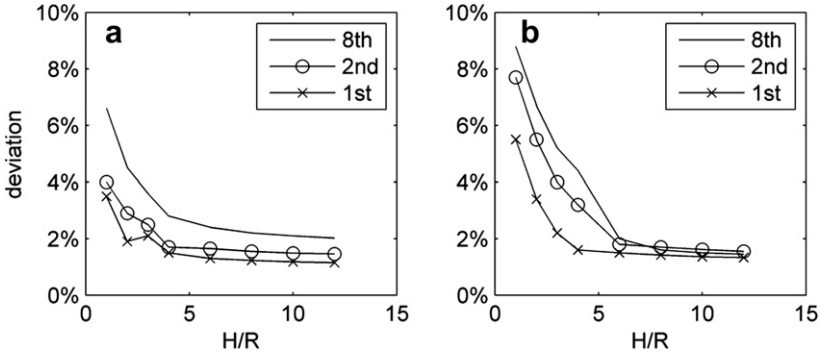

Fig. 9. Deviation of the wake elevation with respect to the turbine height from two locations (a: from mid-span, and b: from blade tip).

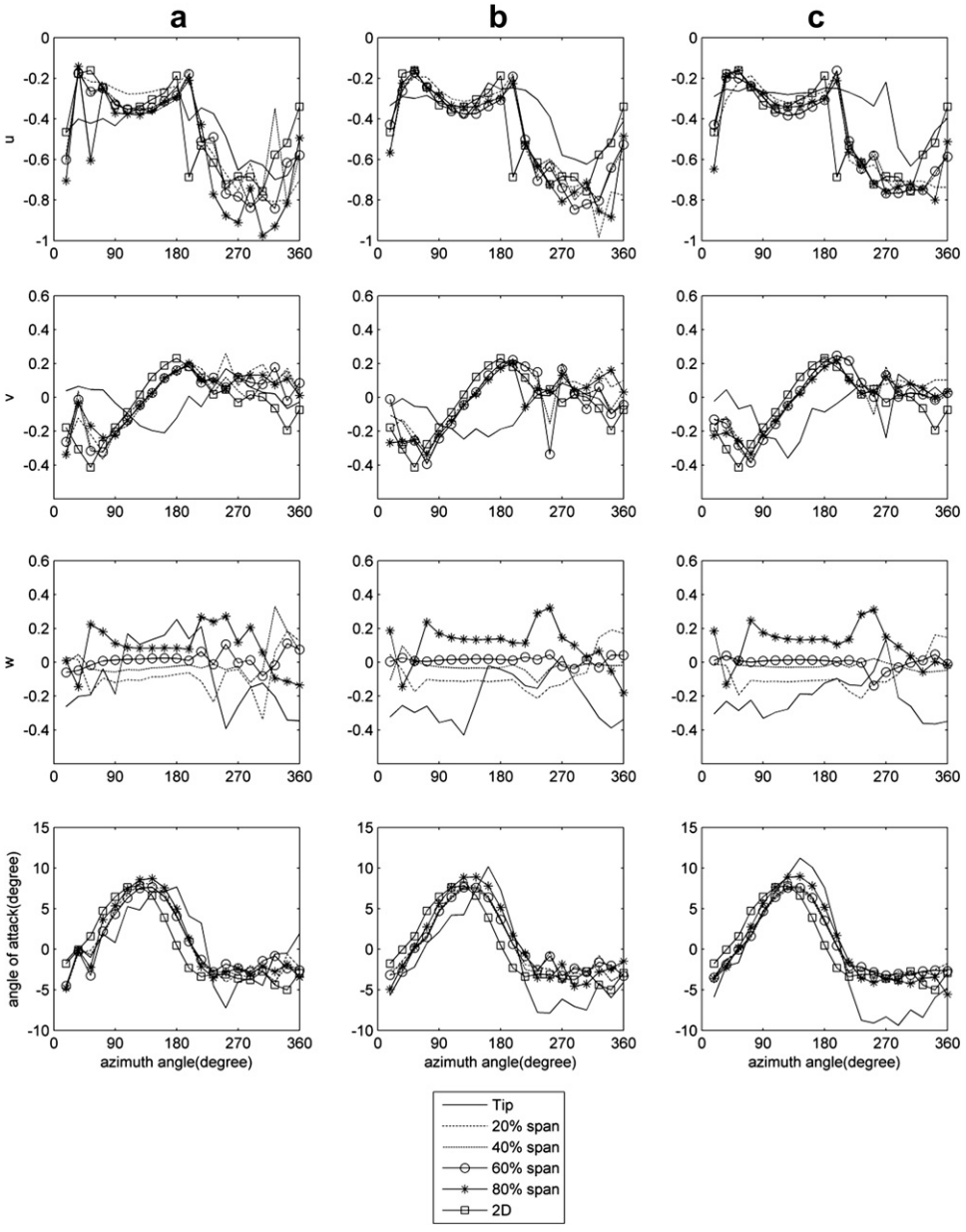

Fig. 10. Induced velocities and angle of attacks of turbines with different heights (a: $H/R = 6$; b: $H/R = 4$; c: $H/R = 1$).

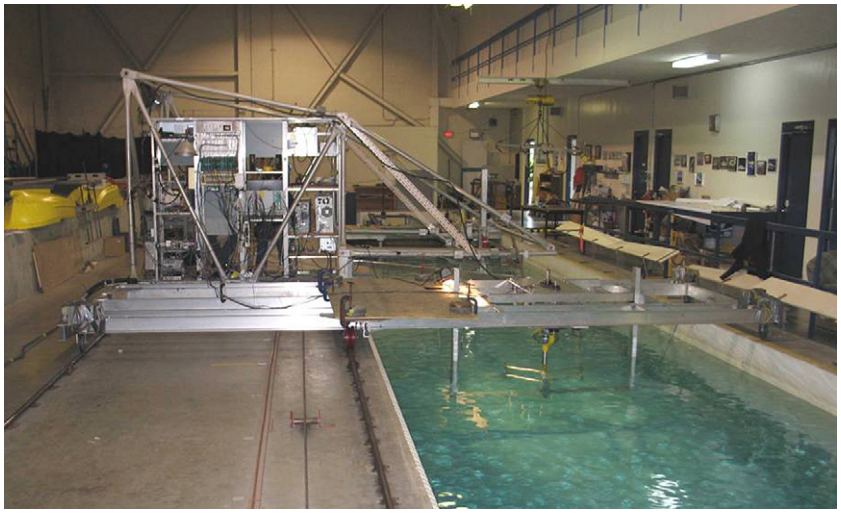

Fig. 11. Experimental setup of the test in the towing tank at the University of British Columbia.

at the University of British Columbia, which is 67 m long, 3.7 m wide and 2.4 m deep and was built in late 1970s. A ship testing carriage was constructed when the tank was built. In order to support the turbine's operation, we designed an additional carriage attached to the original one, as shown in Fig. 11. During the test, the carriage speeds were up to 2 m/s and the turbine's TSR varied from 1.25 to 3.5. The turbine blades are mounted to the central shaft of the turbine via two arms connected at different locations depending on the design. Readers who are interested in experimental setup are suggested to read Li and Calisal [12].

In this section, we mainly discuss the power coefficient of turbines with different arms. Among all arms, we present two in this paper (Fig. 12): Arm type A (heavy arms) and arm type B (light arms). The diameter of the shaft is 3 cm. It is important to know that the clamping mechanism is used for arm type A. This clamping mechanism is designed for adjusting AOA, which significantly increases the drag. Upon removing the blades to examine the power absorbed by the arms, a large portion of the clamping mechanism is also removed, which greatly reduces the parasitic drag compared with that when the blade is mounted. To quantify the effects of arms, we investigated the arm effects by testing the turbine without blades.

3.2. Arm corrections

In order to approximate the power coefficient of the turbine following (11), we present the relationship between TSR and $C_{P,AS}$ for different types arms (Fig. 13). The results show that the power

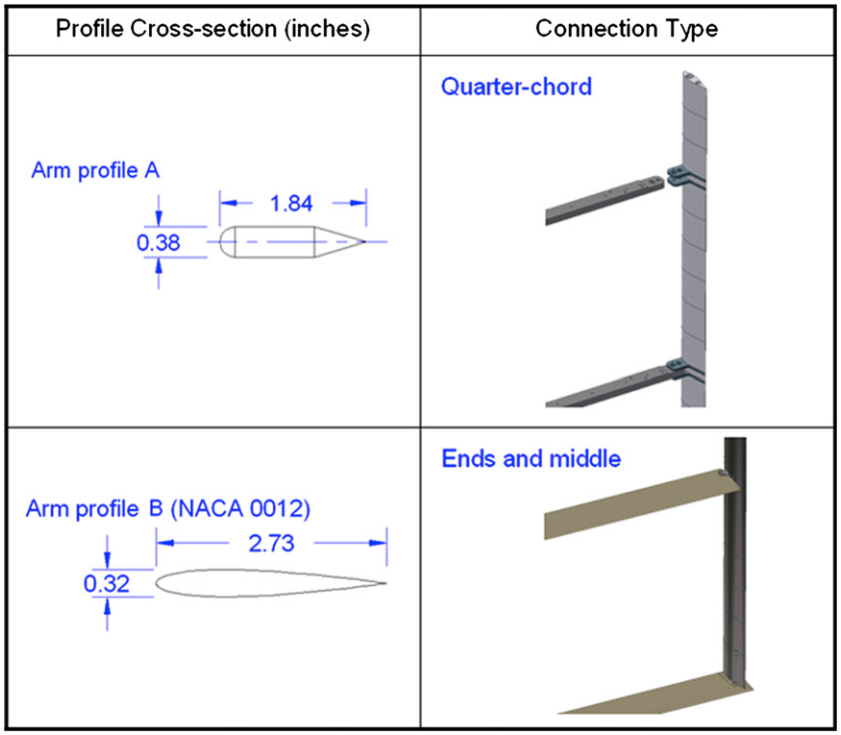

Fig. 12. Configuration of arms Type A and B.

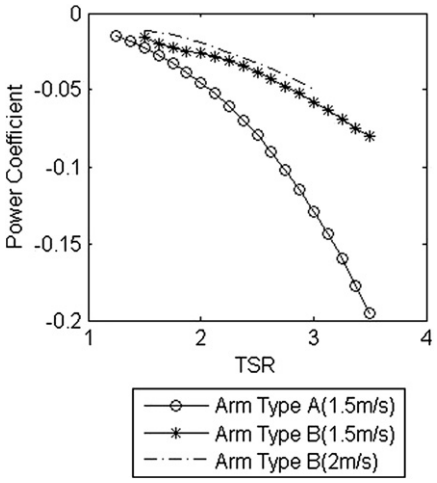

Fig. 13. Power coefficient caused by the arm effects.

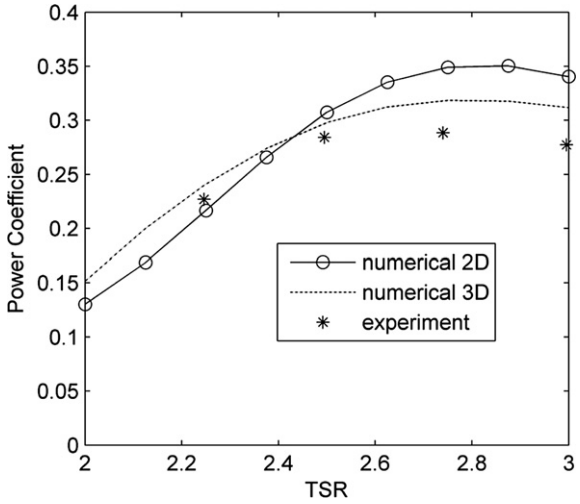

Fig. 14. Power coefficients of a turbine with arm type B.

coefficient contributed by the arm effects of arm type A is the lowest at the same incoming velocity, mainly because the drag coefficient of this arm is more than that of the other two. Furthermore, it shows that the $C_{P,AS}$ of the arm operating at a faster incoming velocity is higher than that of the same arm operating at a slower incoming velocity, due to the change of the Reynolds number.

Considering that the arms are perpendicular to the blade, we assume that the AOA of the arm is 0°, which is theoretically true when the arm is located at the center of the blade. Therefore, we can assume that the power coefficient contributed by the arms, i.e., $C_{P,AS}$, is caused by the drag only. Additionally, the thickness and chord length do not change alone the span. Thus, $C_{P,AS}$ can be written as,

$$C_{P,AS} \approx \frac{\frac{1}{T}\int_0^T \int_0^R C_D \left(r\omega + U_\infty \sin\omega t + \tilde{U}_{\text{induce}}\right)^2 r\omega dr\, dt}{1/2\rho R U_\infty^3} \tag{12}$$

$$T = \frac{2\pi}{\omega} \tag{13}$$

where C_D, $\tilde{U}_{\text{induce}}$, ω and ρ denote drag coefficient, the induced velocity's projection parallel to the chord line of the arm, angular velocity and water density,, respectively. By solving (12) together with (13), we can have $C_{P,AS}$ as a function of TSR, given as follows

$$C_{P,AS} = \kappa_1 \text{TSR}^3 + \kappa_2 \text{TSR}^2 + \kappa_3 \text{TSR} + \kappa_4 \tag{14}$$

The parameters κ_i ($i = 1, 2, 3$ and 4) are determined by the profile of the arm's cross section, the material of the arm, and the Reynolds number, etc. For example, κ_i of arm Type A in 1.5 m/s are (−0.0038, −0.0013, −0.0061, and 0.0022) when the Reynolds number is 160,000.

3.3. Power prediction with arm effect correction

Here, we analyze the power coefficient of a turbine with arm Type B. The specifications of the turbine include that the turbine is a 0.91 m-diameter, three-blade vertical axis turbine, the foil section used for the blades is a NACA $63_{(4)}$-021 section, the solidity is 0.435, the turbine height is 0.5 m, arm type is B, and the incoming flow velocity is 1.5 m/s. We compare the power coefficients obtained using the numerical models with the arm effects correction, (14), with the experimental results (Fig. 14). The results show that the accuracy of the numerical results is quite high. However, because we do not simulate the towing tank's wall, bottom and free surface, which potentially create blockage effects and increase the turbine's power output, the power coefficient obtained with the three-dimensional model is slightly lower than the experimental results. Additionally, it is noted that there is a crossover when TSR is around 2.3. This is mainly because the Reynolds number is the same over the whole computational domain so that the hydrodynamic characteristic does not exactly match the experimental test, although this is acceptable [11].

3.4. End-plate study

With the towing tank setup, we also studied the three-dimensional effects with arms experimentally. We used a typical experimental design to quantify the three-dimensional effects by adding end-plates to the turbine blade so that the test results with end-plates can be considered as two-dimensional results. The specifications of the turbine include that the turbine is a 0.91 m-diameter, three-blade vertical axis turbine, the foil section used for the blades is a NACA 63(4)-021 section, the solidity is 0.435, the turbine height is 0.5 m, the arm type is A, and the incoming flow velocity is 1.5 m/s. In particular, we used two different end-plates, circular and NACA0012 end-plates (Fig. 15), applied to the turbine discussed in Section 3.3. Fig. 16 shows the power coefficients of the turbines with and without end-plates. Good agreement is achieved between the numerical

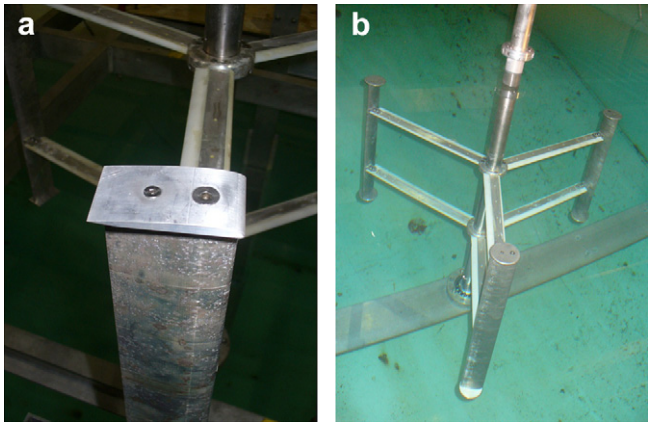

Fig. 15. Turbine with end-plates using the profile of a) NACA0012 and b) circular.

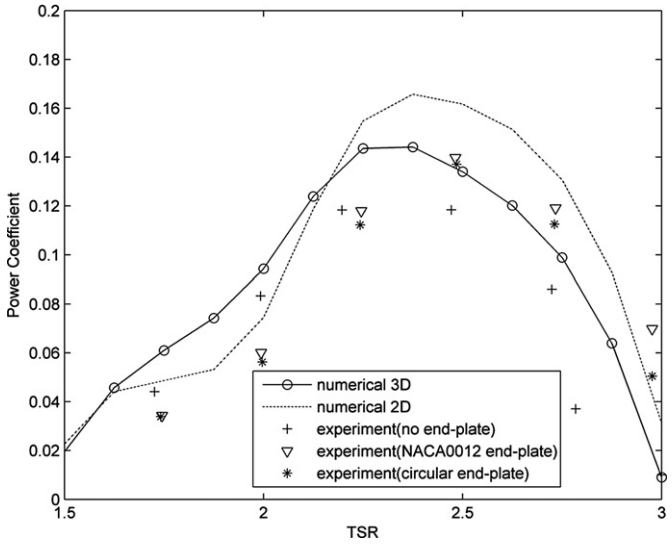

Fig. 16. Power coefficients of turbines with end-plates and arm type A.

results and experimental results. Thus, one can conclude that the arm effects do not increase the three-dimensional effect significantly.

It is noted that the numerical results are higher than the result obtained in the experimental test. This is mainly because high order interactions are not simulated in the numerical model. Other reasons for the noticeable difference between the numerical results and the experimental results include: 1) the quarter span mounting of the foils reduces the length of the working span of the blade; 2) bolt heads are removed, and thus in the assembled case, parasitic drag is larger in tests with those heavier arms. Heavier arms require different blade-arm connection for the purpose of stability, and this connection will significantly increase the drag. Besides, heavier arms will increase the inertia of the whole system so that the dynamic stall may exist; 3) connections are designed for a variable pitch blade, which creates a large space between the blades and arms and produces considerable drag that cannot be measured without the blade been installed; and 4) arm Type A is much heavier than arm Type B; 5) the scale of the end-plate is relatively small.

4. Summary

This paper systematically analyzed the three-dimensional effects in studying vertical axis tidal current turbines. Both two-dimensional and three-dimensional numerical predictions of turbine power coefficient and wake trajectory were compared with experimental results. Fundamental analysis of AOA and induced velocity shows that the higher the height to radius ratio of the turbine, the smaller the three-dimensional effect. We also studied the relationship between the turbine height and these numerical results. The results show that three-dimensional effects are significant when the turbine height is less than two times its radius and can be neglected when the turbine height is more than seven times the turbine radius. However, a three-dimensional model is required for some special purposes such as calculating the vertical flow fluctuation, i.e., the flow fluctuation in the z direction. In addition, arm effects were studied by conducting an experimental test. A quasi-linear relationship is built between the power output of the turbine and the arm effects as a correction for predicting the power output of the turbine. With this new formulation, good agreement was obtained between the numerical results and experimental tests. Additionally, end-plate test results were analyzed, which suggest that a combination of three-dimensional effects and arm effects are rather trivial. For those turbine designers in the initial design stage, because the computational time of the three-dimensional model is more than thirty times that of the two-dimensional model, one can say that the two-dimensional model is more cost-effective than the three-dimensional model.

However, the numerical model used in this paper simulates an ideal condition. Practical conditions such as boundary layer profile, turbulence, and free surface and bottom effects are not discussed. Future work is desired to analyze these effects in the three-dimensional model. Besides, towing tank tests were conducted close to the free surface and tank bottom. Although acceptable agreement was achieved between the numerical prediction and the experimental results, the missing representations of free surface and tank bottom indicate that the agreement should be improved further. The effects of hydrodynamic interactions between the arm, shaft and blade shall be investigated theoretically so as to lessen the power reduction caused by such effects.

Another worth noting point is the arm effect correction [10–12]. It is clear that the derivation is based on perturbation method and by assuming that the AOA of the arm is is 0°. Practically, due to the effects of the induced velocity, AOA shall periodically fluctuate if the arm is not connected with the middle plane of the blade. Furthermore, the higher order term of the interaction between arm, shaft and blades will also affect the arm effects although it is not significant in the case studies in this paper. In the future, we shall study both the AOA fluctuation and the higher order interaction in a more generic scenario.

Acknowledgements

The analysis of this work was conducted under assistance of several generous fellowships agencies which are acknowledged here, such as: National Science and Engineering Research Council, Society of Naval Architects and Marine Engineers, Institution of Electronic and Electric Engineers, American Society of Mechanical Engineers and International Society of Ocean Polar Engineers. The authors would also like to thank Western Economic Diversification and Blue Energy Canada for supporting the experimental test.

References

[1] Lang C. Harnessing tidal energy takes new turn. IEEE Spectrum 2003;40:13–4.
[2] Garret C, Cummins P. The efficiency of a turbine in a tidal channel. Journal of Fluid Mechanics 2007;588:243–51.
[3] Li Y, Lence BJ, Calisal SM. Modeling the energy output from an in-stream tidal turbine farm. Journal of Computers 2009;4(4):288–94.
[4] Van Walsum E. Barrier to tidal power: environmental effects. International Water Power and Dam Construction 2003;55:38–42.
[5] Battern WMJ, Bahaj AS, Molland AF, Chaplin JR. Hydrodynamics of marine current turbines. Renewable Energy 2006;31:249–56.
[6] Coiro DP, De Marco A, Nicolosi F, Melone S, Montella F. Dynamic behaviour of the patented kobold tidal current turbine: numerical and experimental aspects. Acta Polytechnica 2005;45:77–84.
[7] Li Y, Calisal SM. Numerical analysis of the characteristics of a vertical axis water current turbine. Renewable Energy 2010;35(2):435–42.
[8] Davis BV. Water turbine model trials. Nova Energy Limited for NRC Hydraulics Laboratory NEL-002; 1980. 120pp.
[9] Ponta FL, Jacovkis PM. A vortex model for Darrieus turbine using finite element techniques. Renewable Energy 2001;24:1–18.
[10] Antheaume S, Maitreb T, Achard J. Hydraulic Darrieus turbines efficiency for free fluid flow conditions versus power farms conditions. Renewable Energy 2008;33:2186–98.
[11] Li Y, Calisal SM. Preliminary results of a discrete vortex method for individual marine current turbine. Proceedings of 26th the International Conference on Offshore Mechanics and Arctic Engineering 2007;5:589–98.
[12] Li Y, Calisal SM. A new discrete vortex method for simulating a stand-alone tidal current turbine modeling and validation. Journal of Offshore Mechanics and Arctic Engineering 2010;132(3). doi:10.1115/1.4000499.
[13] Calcagno G, Salvatore F, Greco L, Moroso A, Eriksson H. Experimental and Numerical Investigation of an Innovative Technology for Marine Current

Exploitation: The Kobold Turbine. Proceedings of the International Offshore and Polar Engineering Conference, 2006. p. 323–30.
[14] Strickland JH, Webster BT, Nguyen T. Vortex model of the Darrieus turbine: an analytical and experimental study. Journal of Fluids Engineering 1979;101: 500–5.
[15] Anderson DJ. Fundamentals of aerodynamics. 4th ed. New York: McGraw-Hill; 2005.
[16] Templin R. Aerodynamic performance theory for the NRC vertical axis wind turbine. Technical Report LTR-LA-160, National Research Council Canada, 1974. 102pp.
[17] Strickland JH. The Darrieus turbine: a performance prediction model using multiple streamtubes. Sandia National Lab Report SAND75-043, 77pp; 1976.
[18] Van Dyke M. Perturbation methods in fluid mechanics. Stanford: CA Parabolic Press; 1975.